Cement and Concrete Research 118 (2019) 111–119

Contents lists available at ScienceDirect

Cement and Concrete Research

journal homepage: www.elsevier.com/locate/cemconres

Service life and life cycle assessment of reinforced concrete systems with limestone calcined clay cement (LC3)

Radhakrishna G. Pillai*, Ravindra Gettu, Manu Santhanam, Sripriya Rengaraju, Yuvaraj Dhandapani, Sundar Rathnarajan, Anusha S. Basavaraj

Department of Civil Engineering, Indian Institute of Technology Madras, Chennai, India

ARTICLE INFO

Keywords:
Concrete
Alternate binders
Chloride diffusion
Corrosion
Service life
Life-cycle assessment
CO_2 emissions

ABSTRACT

This paper presents data on the chloride diffusion coefficient (D_{cl}), ageing coefficient (m) and chloride threshold (Cl_{th}) related to seven concrete mixes (four M35 and three M50) with OPC, OPC + PFA (pulverised fuel ash) and limestone-calcined clay cement (LC3). Using these, the service lives of a typical bridge pier and girder with the PFA and LC3 concrete were found to be much higher than those with OPC concrete of similar strength. From life-cycle assessment, the CO_2 footprint of PFA and LC3 concrete were found to be significantly lower than those of OPC concrete of similar strength. Further, the CO_2 emissions per unit of concrete per year of estimated service life, as a combined indicator of service life and carbon footprint, are similar for concrete with PFA and LC3, which are much lower than that with OPC.

Symbols and notations

%bwob	Percentage by weight of binder
%bwoc	Percentage by weight of concrete
Cl_s	Surface chloride concentration [%bwoc]
Cl_{th}	Chloride threshold [%bwoc]
d	Cover depth [mm]
D_{365d}	Diffusion coefficient determined at the age of 365 days [m^2/s]
D_{cl}	Chloride diffusion coefficient [m^2/s]
D_{ref}	Chloride diffusion coefficient at t_{ref} [m^2/s]
LC3	Limestone calcined clay cement
LCA	Life cycle assessment
m	Ageing coefficient for the chloride diffusion coefficient
M35	Concrete with characteristic cube compressive strength of 35 MPa at 28 days
M50	Concrete with characteristic cube compressive strength of 50 MPa at 28 days
n	Number of time steps
N_f	Number of instances of failure
OPC	Ordinary portland cement
P_f	Probability of failure
PFA	Pulverised fuel ash
SCMs	Supplementary cementitious materials
QST	Quenched and self-tempered
RC	Reinforced concrete
t	Age of the structure [years]
t_{ref}	Reference time [years]
$\sigma(t)$	Electrical conductivity of concrete at time t [mS/m]
σ_{ref}	Electrical conductivity of concrete at t_{ref} [mS/m]

1. Introduction

1.1. Background

Chloride-induced corrosion is a major cause of deterioration in reinforced concrete (RC) structures, leading to premature failure and economic burden due to frequent repair and maintenance [1,2]. The consequent reduction of the service life can lead to socio-economic losses and increase in the environmental impact due to the higher raw material requirement and CO_2 emissions per year of life. Further, frequent repair and maintenance increase the consumption of raw materials and other resources, which in turn increases the total CO_2 footprint of the structure during its life cycle. Along these lines, supplementary cementitious materials (SCMs), such as fly ash, have the potential of enhancing durability, as well as reducing the environmental impact of concrete. The recognition of the importance of service life considerations in structural design has led to a steady shift from prescriptive- to performance-based specifications of concrete [3,4]. Recently, the performance of a ternary-blend made of Portland cement clinker,

* Corresponding author.
E-mail address: pillai@iitm.ac.in (R.G. Pillai).

https://doi.org/10.1016/j.cemconres.2018.11.019
Received 27 March 2018; Received in revised form 30 July 2018; Accepted 30 November 2018
Available online 23 December 2018
0008-8846/

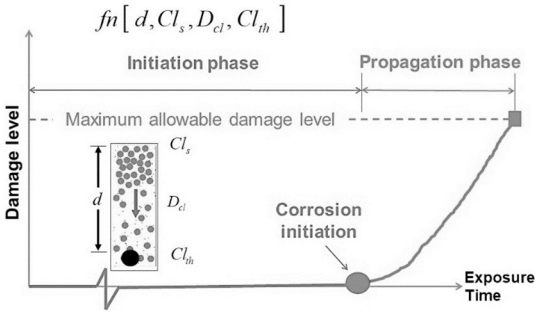

Fig. 1. Various stages of service life and influencing parameters (adapted from [11]).

limestone and calcined clay, called limestone calcined clay cement (denoted as LC3), has been assessed extensively for its advantages over ordinary Portland cement (OPC) [5–9]. It has shown promise in significantly enhancing the chloride resistance of concrete, when compared to other concrete mixes of similar compressive strength made with OPC only or OPC with fly ash [10] The present work assesses the benefits of using LC3 in terms of the increase in estimated service life and decrease in total CO_2 emissions during the service life of RC systems exposed to chlorides, and compares its performance with binders having 100% OPC and '70 % OPC + 30 % fly ash'.

1.2. Service life estimation

Service life, which is compromised by the corrosion of steel reinforcement due to chloride attack, can generally be divided into the initiation and propagation phases; see Fig. 1 [11]. During the former, chlorides from the environment traverse the cover concrete (mainly driven by diffusion) to reach the surface of the reinforcement bar (rebar). The chloride concentration at the steel-cementitious interface increases gradually and reaches a level, known as chloride threshold, Cl_{th}, at which corrosion initiates [12]. During the propagation phase, the corrosion progresses and induces expansion, and the concrete cover eventually cracks and/or spalls, resulting in partial failure or repair/replacement of the structural element. Due to the presence of multiple structural cracks, corrosion of multiple rebars, variations in the ambient climate conditions, and microclimate at the steel-cementitious interface, the estimates of the propagation periods could be misleading. Hence, it is usual to assume a relatively short and conservative estimate for the corrosion propagation period.

In service life estimation, it is common to conservatively assume the service life to end when corrosion initiates (i.e., end of the initiation phase in Fig. 1) [13]. The duration of this phase is governed by the surface chloride concentration (Cl_s), the chloride diffusion coefficient (D_{cl}), the ageing coefficient for D_{cl} (m), the cover depth (d) and the chloride threshold (Cl_{th}). The parameters D_{cl} and m depend on the type of binder, concrete composition, curing and the exposure condition, whereas Cl_{th} is a characteristic of the steel-cementitious interface. For estimating the service life and comparing the performance of various binders, a rational approach considering the influence of all these critical parameters is required.

1.3. CO_2 emissions

The major impacts of concrete construction are the raw material consumption, which influences the depletion of natural resources, and the CO_2 emissions, which govern global warming. It is said that CO_2 emissions from cement production contribute to 5–8% of the total global CO_2 emissions [8] and this is expected to increase in line with the predicted quadrupling of the cement consumption by the year 2050 [14]. In this scenario, the use of more durable concrete made with abundantly available local raw materials, with low embodied energy and CO_2 emissions, would have significant benefits for the sustainability of concrete construction. The life cycle assessment (LCA) methodology is used here to estimate the CO_2 emissions that can be attributed to each of the concrete mixes considered. Since blended binders can influence both durability and environmental impact, the present work combines service life estimation and carbon footprint by computing the CO_2 emissions per year of expected service life, as done by Van den Heede and De Belie [15]. This is also along the lines of the building material sustainability potential proposed by Müller et al. [16].

2. Research significance

Limestone calcined clay cement (LC3) is being recognized as a suitable candidate material for the development of durable concrete with low environmental impact. This paper provides a holistic assessment of the suitability of LC3, by combining both service life and CO_2 footprint as significant parameters. Experimental data on chloride ingress and corrosion initiation have been employed for the service life estimates, which have been linked to the estimates of the CO_2 footprint of LC3 concrete. Comparisons are made with concrete of similar strength grades made with OPC, and a blend of OPC and 30% fly ash. Case studies of a bridge pier and a bridge girder are presented to illustrate the influence of binder choice on the probabilistic service life and the carbon footprint/year of service life.

3. Methodology used

This section describes the materials used and experimental methodology for obtaining the input parameters (i.e., D_{cl}, m and Cl_{th}) needed to estimate the probabilistic service life of a structural element made with these materials. Also, the approach and parameters used to calculate the total CO_2 emissions are discussed so that the CO_2 footprint per year of service life can be estimated.

3.1. Materials and mixture details considered

The chemical composition and relevant properties of the materials used in the study are presented in Table 1. Table 2 provides the mixture proportions and various properties of the concrete assessed in the study. A 53 Grade OPC (containing 7.2% C_3A content), conforming to Indian Standard 12,269 [17], was used. The PFA concrete (where PFA stands for pulverised fuel ash) was made using a blend of OPC and Class F fly ash (at 30% replacement of OPC). LC3, with a composition of 50%

Table 1
Chemical composition and properties of materials used.

Composition	OPC	Class F Fly ash	LC3		
			Clinker	Calcined clay	Limestone
CaO	64.59	1.28	63.81	0.09	48.54
SiO_2	19.01	59.32	21.12	58.43	10.07
Al_2O_3	4.17	29.95	5.24	24.95	1.74
Fe_2O_3	3.89	4.32	3.41	5.08	1.62
MgO	0.88	0.61	3.06	0.19	0.467
Mn_2O_3	–	–	0.06	–	0.035
Na_2O	0.16	0.16	0.32	0.05	–
K_2O	0.59	1.44	0.19	0.21	0.13
TiO_2	0.23	–	0.10	1.41	0.206
SO_3	1.70	0.16	0.63	–	0.01
LOI	1.40	–	0.98	9.58	37.09
Specific gravity	3.16	2.77	–	2.67	2.63
				3.01	
Blaine specific surface area (m^2/kg)	340	330		520	
Median grain size d_{50} (μm)	18	23		11	

Table 2
Mixture proportions for the different concrete mixes studied and their relevant parameters.

Ingredients and properties of concrete		M35				M50		
		OPC-1	PFA-1	LC3-1S	LC3-1P	OPC-2	PFA-2	LC3-2
Binder type		OPC	OPC + PFA	LC3	LC3	OPC	OPC + PFA	LC3
Binder content (kg/m^3)		310	360	310	360	360	380	340
Water content (kg/m^3)		155	162	155	162	144	133	136
Water-binder ratio		0.5	0.45	0.50	0.45	0.4	0.35	0.4
Fine aggregate content (kg/m^3)		695	721	708	687	703	699	704
Coarse aggregate content (kg/m^3)	10 mm down	496	463	491	476	477	475	488
	20 mm down	744	694	736	715	716	713	732
28-day compressive strength (MPa)	mean	45.4	37.6	38.8	40.7	60	54.6	56.7
	cov	0.01	0.04	0.004	0.005	0.03	0.03	0.004
Diffusion coefficient at 365 days	mean	18.7	3.5	3.3	1.3	15.6	1.9	1.7
($\times 10^{-12}$ m^2/s)	cov	0.34	0.20	0.08	0.12	0.17	0.22	0.07
Electrical conductivity mS/m	at 28 days	11.87	7.79	0.65	0.51	9.79	4.67	0.51
	at 90 days	10.19	3.40	0.39	0.27	8.38	2.46	0.25
	at 365 days	4.87	1.03	0.18	0.14	6.23	1.06	0.14
Ageing coefficient, m	μ	0.26	0.7	0.5	0.53	0.17	0.55	0.54
	cov	0.3	0.14	0.27	0.14	0.31	0.15	0.19
Cl_{th}	μ	0.06	0.05	0.02	0.03	0.07	0.05	0.02
(% bwoc)	cov	0.28	0.32	0.39	0.39	0.28	0.32	0.39
Total CO_2 emissions/m^3 of concrete (kgCO_2 eq./m^3)		335	290	255	280	380	300	270

%bwoc - % by weight of concrete (converted from %bwob, as per the total binder content).
cov - coefficient of variation.

clinker, 31% calcined clay, 15% crushed limestone and 4% gypsum, obtained from an industry-scale trial production, was used; further details of LC3 can be found elsewhere [7].

Seven concrete mixes in two strength categories (i.e., M35 and M50) were adopted for the study based on typical concrete used in practice. As shown in Table 2, in the M35 category, OPC-1 and PFA-1 concrete were proportioned using different binder contents and water-binder ratios to attain a 28-day cube characteristic strength of 35 MPa. In the same category, two LC3 concrete mixes (i.e., LC3-1S and LC3-1P) were proportioned such that LC3-1S concrete had similar strength as OPC-1 and PFA-1, and LC3-1P concrete had similar mixture proportions as PFA-1. In the M50 category, OPC-2, PFA-2 and LC3-2 were proportioned using different binder contents and water-binder ratios to attain the characteristic strength of 50 MPa. In all cases, the initial slump of 80–120 mm was obtained by adjusting the dosage of a polycarboxylic ether (PCE) based superplasticiser, in the range of 0.2–1% solids by weight of the binder.

3.2. Determination of the service life parameters and service life

3.2.1. Chloride diffusion coefficient (D_{cl})

Fick's 2nd law of diffusion can be used to model the chloride ingress through the cover concrete. Using this, the chloride concentration $Cl(x, t)$ at depth x, from the exposed surface at exposure time t, can be determined as follows:

$$Cl(x,t) = Cl_s \cdot \left(1 - \mathrm{erf}\left(\frac{x}{2\cdot\sqrt{D_{cl}\cdot t}}\right)\right) \quad (1)$$

where, Cl_s is the surface chloride concentration; the terms Cl_s and $Cl(x, t)$ are expressed in % by weight of concrete (%bwoc); D_{cl} is the apparent chloride diffusion coefficient in m^2/s, and erf() is the mathematical error function. The effect of adding SCMs on the reduction of D_{cl} and increase in the time required for the building-up of Cl_s on the concrete surface has been discussed extensively in the literature [18–20]. These phenomena are mainly attributed to the refined pore structure and increased chloride binding in the blended systems, when proportioned and cured appropriately.

In order to determine D_{cl} for the different concrete mixes, the bulk diffusion test has been performed on 100 × 200 mm cylindrical specimens, which had been cured in a mist room for a period of one year. In order to limit the effects of the microstructure evolution on the chloride ingress, it was preferred to determine the diffusion coefficient after 365 days of curing (denoted as D_{365d}). The cylindrical specimens were initially coated with epoxy, and after the epoxy had hardened, the specimens were sliced into halves, each of 100 mm thickness. The specimens were carefully sawn to avoid any damage to the epoxy coating. For each concrete, two slices were immersed in 2.8 M NaCl solution for a period of 56 days, after conditioning them with saturated calcium hydroxide solution, as per ASTM C1556 [21]. Chloride profiles were obtained by sampling concrete powder extracted over 25 mm from the concrete surface (i.e., at 0–1, 1–2, 2–3, 3–4, 4–6, 6–8, 8–10, 10–12, 12–15, 15–18, 18–21, and 21–25 mm). The powder was tested, as per SHRP 330 [22], for acid soluble chlorides to estimate the variation in the chloride content as a function of depth from the exposed surface. Then, the mean and coefficient of variation (cov) of D_{365d} were determined using the profile obtained (see Table 2).

3.2.2. Ageing coefficient (m) and reduction of D_{cl}

The ageing coefficient (also known as the decay constant), m, helps to account for the reduction in D_{cl} over time, due to the evolution of the microstructure of the hardened binder phase and the chloride binding capacity. The consequent change in D_{cl} can be expressed as [23]:

$$D_{cl,\ t} = D_{cl,\ ref} \left(\frac{t_{ref}}{t}\right)^m \quad (2)$$

where, $D_{cl,t}$ and $D_{cl,ref}$ are the diffusion coefficients at exposure time t, and reference time t_{ref} (e.g., 365 days), respectively. Concrete with SCMs have been found to exhibit steady reduction in D_{cl} as time progresses [24]; m-values for concrete with fly ash vary over a range of 0.4 to 0.8 [25].

Two approaches to quantify m have been reported in the literature. A direct method is based on the experimental determination of the evolution of D_{cl} over prolonged periods of exposure (say, several years) and the subsequent determination of m through regression analysis of Eq. (2). However, this requires exposure to chlorides over several years along with assessment involving profiling. In the present study, an indirect method has been adopted based on the work by Andrade et al.

[23], considering that the electrical conductivity of concrete σ evolves as follows:

$$\sigma_t = \sigma_{ref}\left(\frac{t_{ref}}{t}\right)^m \quad (4)$$

where, σ_t and σ_{ref} are the electrical conductivities at exposure time t, and reference time t_{ref} (e.g., 28 days); and m is the ageing coefficient based on conductivity. In this study, the electrical conductivity has been determined at 28, 90 and 365 days as per ASTM C1760 [26], and was analysed through regression to obtain the values of m (see Table 2). For calculating the ageing coefficient, electrical conductivity was considered as an indicator of the change in the resistance to chloride ingress [26–28]. Since this approach relates m to the development of the physical structure of the hardened binder phase and does not consider the change in diffusivity due to chloride binding, it leads to a conservative estimate [23].

3.2.3. Chloride threshold (Cl_{th})

The chloride threshold, Cl_{th}, is highly dependent on the type of steel and binders; along with other environmental and material factors [12]. Typically, due to the significant consumption of $Ca(OH)_2$ in blended cement systems, there could be a reduction in the pH buffering capacity at the steel-cementitious interface, leading to lower values of Cl_{th} [29].

Lollipop-type specimens (100 mm long and 30 mm diameter) were used to determine Cl_{th} (see Fig. 2). The specimens were prepared with an 8 mm diameter and 70 mm long QST steel rebar embedded in mortar with the proportions of water:binder:sand ratio as 0.5:1:2.75. Polypropylene centrifuge tubes were used as moulds for the specimens, which were demoulded after 24 h and cured in a mist room (at 25 ± 2 °C) for 14 days and then immersed in simulated pore solution (SPS) with 3.5% NaCl; a litre of SPS contained 10.4 g of NaOH, 23.2 g of KOH and 0.3 g of $Ca(OH)_2$ in distilled water. After that, the specimens were subjected to wet-dry cycles (i.e., two days of wetting followed by five days of drying) using SPS with 15% NaCl at constant room temperature (at 25 ± 2 °C). At the end of each wet period, linear polarization resistance (LPR) tests were conducted in a three-electrode cell by sweeping the potential from −15 mV to +15 mV versus the open circuit potential (OCP), at a scan rate of 0.1667 mV/s. A saturated calomel electrode (SCE) was used as the reference and nichrome mesh was used as the counter electrode. The polarization resistance (R_p) was monitored until the polarization resistance dropped below 10,000 Ω·cm^2 [30], at which point corrosion is deemed to have initiated in the rebar. After this, the specimen was split along the rebar and the chloride concentration in the powder collected from the interfacial region was determined using the acid-soluble chloride analysis [22], and taken as Cl_{th}. For service life estimates, the mean and coefficient of variation of the Cl_{th} observed from 10 specimens in each case (OPC, PFA, and LC3) were used.

3.2.4. Service life estimation

The probabilistic service life of a reinforced concrete system is estimated in this study in terms of the time taken for the initiation of rebar corrosion, i.e., when the concentration of chloride at the level of embedded steel reaches the chloride threshold (Cl_{th}). A MATLAB program was written to estimate the service life using the solution of Fick's 2nd law of diffusion (see Eq. (1)). The input parameters were the clear cover depth (d), chloride diffusion coefficient at 28 days (D_{28d}), ageing co-efficient (m), surface chloride concentration (Cl_s), chloride build-up rate, maximum Cl_s and chloride threshold (Cl_{th}). The D_{28d} was obtained from the bulk diffusion test and it was assumed that the D_{cl} remained constant after the concrete reached the age of 25 years. The d, D_{28d} and Cl_{th} were considered as random variables (as per the mean and coefficient of variation given in Table 2); the coefficient of variation for d was assumed to be 10%. 1000 random realizations were simulated and the amount of chloride concentration at the level of steel (C_x) was calculated in each case. For every time step (say, every year), the calculated C_x-values were compared with the randomly generated Cl_{th} values, and the number of instances of failure (N_f) (i.e., $C_x \geq Cl_{th}$) was computed to get the probability of failure (P_f) for corrosion initiation. Then, the cumulative probability of failure for the n^{th} year was obtained by adding N_f for all n time steps and dividing by 1000n. These cumulative P_f-values were used to generate the cumulative distribution functions (CDFs) of corrosion initiation time.

3.3. Life cycle assessment (LCA)

The four major steps in LCA [31] are: i) system boundary definition, ii) inventory analysis, iii) impact assessment, and iv) comparative analysis (Fig. 3). The system boundary defines the scope of the analysis, and in this study the ground-to-gate or mine-to-gate system has been considered. The inventory analysis was done using a typical cement plant as the primary source of data and several secondary sources of data, such as the database from ecoinvent, Environmental Policy Act (EPA), and the Intergovernmental Panel on Climate Change (IPCC) report. For the environmental impact assessment, CO_2 emission is considered as the index, and the conversion factors used are given in Table 3; for processes or materials for which conversion factors were not available, the corresponding emission has been modelled with the widely-used SimaPro software v8.0.5.13 (Pré Consultants 2016). All processes from the extraction of raw materials, production of electricity and transportation (fuels, cement, fine aggregates, coarse aggregates,

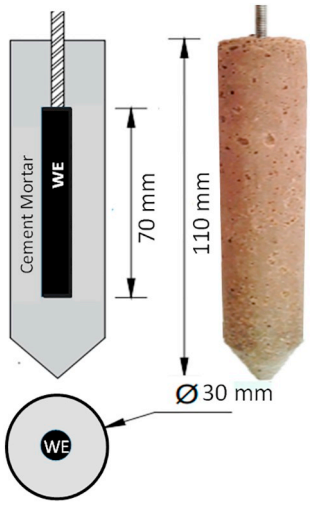

Fig. 2. Specimen for chloride threshold assessment.

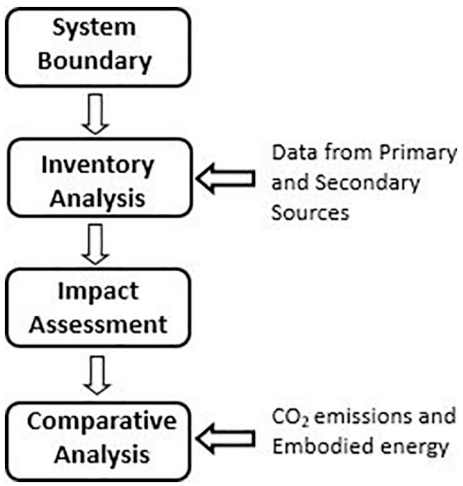

Fig. 3. Steps involved in life-cycle assessment.

Table 3
CO_2 conversion factors for clinker, cement, concrete for LCA (Ground-to-Gate system).

Material type	Materials/processes	Conversion factors for calculating CO_2 emissions ($kgCO_2eq./kg$)*	Source			
			Ecoinvent [46]	IPCC & EPA [47]	Cement plant data	Modelled in SimaPro [48]
Clinker	Limestone (Ext + Cal)	0.5179	✓		✓	
	Clay (Ext)	0.00294	✓			
	Coal (Ext + Comb)	0.552	✓	✓		
	Lignite (Ext + Comb)	0.0763	✓	✓		
	Pet coke (Ext + Comb)	0.294	✓	✓		
	Diesel (Ext + Comb)	0.569	✓	✓		
	Plastics (Comb)	1.21		✓		✓
	Tyres (Comb)	2.24		✓		✓
	Other alternative fuels (Comb)	1.44		✓		✓
	Paint sludge (Comb)	0.98		✓		✓
	Electricity production	1.38[a]	✓		✓	
	Truck transportation (including diesel consumption)	0.092[b]	✓		✓	
Cement	Clinker	0.85				✓
	Limestone	0.00219	✓			
	Gypsum	0				
	Electricity production	1.38[b]	✓			
	Truck transportation (of gypsum, fly ash, limestone)	0.092[a]	✓			✓
	Fly ash	0				
	Calcined clay (Cal)	0.127				✓
Concrete	Cement (OPC)	0.82				✓
	Cement (LC3)	0.554				✓
	Fine aggregates (Ext)	0.00419	✓			
	Coarse aggregates (Ext)	0.00419	✓			
	Water	0.000658	✓			
	Truck transportation of cement and aggregates	0.0924[b]	✓			
	Electricity production	1.38[a]	✓			

Abbreviations: Cal – Calcination, Ext – Extraction, Comb – Combustion.
* Exceptions are indicated: a - $kgCO_2$ eq./kWh, b - $kgCO_2$ eq./t-km.

PFA) up to the processes in the production of concrete in the RMC plant were considered. Fuel consumption for transportation is based on trucks or bulkers with 23-t freight capacity. The impact of truck transportation has been taken from the ecoinvent database, which includes all direct and indirect emissions due to fuel extraction and consumption, manufacturing and maintenance of truck, road construction, etc.

The primary data was collected from a cement plant situated in the limestone-rich region of Ariyalur, in Tamil Nadu, India. For the CO_2 footprint calculation of the transportation distances, it was considered that the concrete mixes were batched and mixed at a ready-mix concrete plant in Chennai, at approximately 300 km from the cement plant at Ariyalur. Based on the actual practices in the region, it was assumed that sand was brought from Villupuram (192 km from Chennai), coarse aggregate from Kanchipuram (75 km from Chennai), and clay for LC3 from Dharmapuri (104 km from Ariyalur). Based on the Thermogravimetric Analysis (TGA) and Differential Scanning Calorimetry (DSC) tests conducted on different clay samples, the calcination of the clay in a kiln with an efficient heat recovery system was conservatively estimated to be 2.6 MJ/kg (considering 30% energy loss and 13% mass loss during calcination). Fuel used in the calcination was assumed to be same as that used in clinkerization. Electricity required for calcining in the rotary kiln was assumed to be 0.04 kWh/kg of clay. The total $kgCO_2$ eq. emissions that can be attributed to 1 m^3 of concrete was calculated for the different concrete mixes using the conversion factors given in Table 3, following the framework suggested by Gettu et al. [32].

4. Results and discussion

The various parameters needed for the service life estimation have been obtained using the procedures explained in the previous sections and are discussed in the following.

4.1. Chloride diffusion coefficient (D_{cl})

Chloride profiles obtained from the bulk diffusion tests on the seven concrete mixes are presented in Fig. 4(a) and (b). The OPC mixes showed higher rates of chloride ingress in both categories (i.e., M35 and M50), with a profile that is distinctly different from those of the PFA and LC3 mixes. This can be attributed to the less porous microstructure and the high ionic resistance of the binder phases in PFA and LC3 concrete [33,34]. The differences in the surface chloride concentration are mainly governed by the near surface porosity of the concrete. The LC3-1S, LC3-1P, LC3-2 and PFA-1 concrete exhibited low porosity and lower pore sizes, resulting in lower surface chloride concentrations [10] in spite of the same exposure. Moreover, the lower slope for the OPC systems suggests that the chloride transport is mainly diffusion driven and dependent on the concentration gradient. Fig. 4(a), corresponding to the M35 concrete, shows that the chloride concentrations are low in both LC3-1P (with mixture proportion similar to PFA-1) and LC3-1S (with lower binder content and high w/b). Similarly, among the M50 concrete (see Fig. 4b), OPC-2 experiences higher ingress of chlorides than PFA-2 and LC3-2, both of which seem to have similar resistance to chloride.

Using regression analysis of an error function solution of Fick's 2nd law of diffusion, the chloride diffusion coefficients (D_{365d}) were determined from the chloride profiles, and are presented in Table 2, in terms of mean values and coefficients of variation. In line with trends seen in the observed chloride concentrations, the diffusion coefficients of the OPC mixes were higher (by an order of magnitude) than those with PFA and LC3. The diffusion coefficients of the PFA and LC3

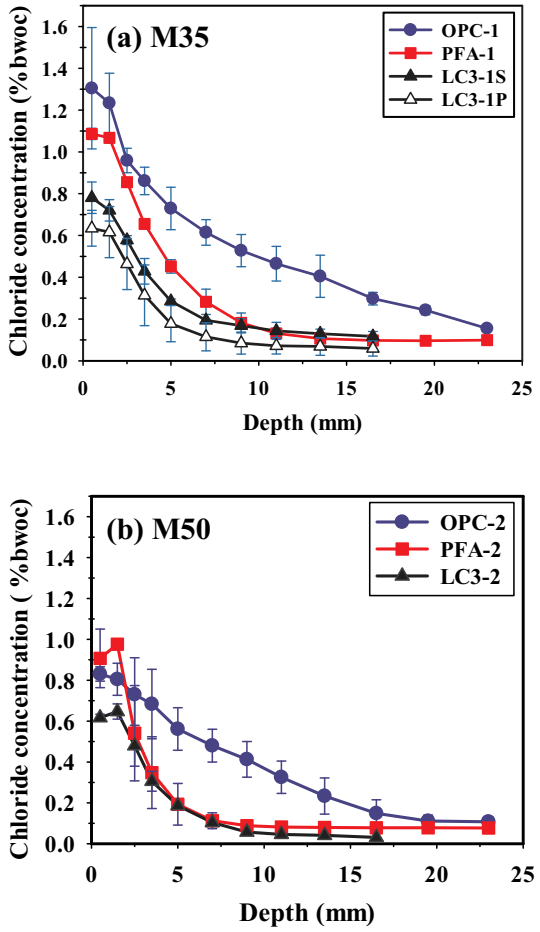

Fig. 4. Chloride profiles in the concrete mixes after 56 days of exposure to chloride solution, (a) M35 and (b) M50 concrete (%bwoc = % by weight of concrete).

concrete are similar in each category, except for LC3-1P, which exhibits the lowest diffusion coefficient.

The differences in diffusivity can be explained based on the kinetics of microstructural development and reactivity potential of the three binders. The similar performance of PFA-1 and LC3-1S in the M35 category, and PFA-2 and LC3-2 in the M50 category can be attributed to the lower w/b in the PFA mixes. On the other hand, in mixtures with similar proportions, the higher reactivity of calcined clay has a dominant impact on the chloride transport, resulting in a lower diffusion coefficient for LC3-1P than for PFA-1. The observed data strongly suggest that the interconnectivity of pores, pore size, and chloride binding capacity play significant roles in reducing the diffusion coefficient of blended cement systems.

4.2. Ageing coefficient (m)

Table 2 gives the electrical conductivity of the seven concrete mixes at 28, 90 and 365 days of curing. The change in electrical conductivity mainly reflects the evolution of the interconnected pores in the hydrated cement paste and voids in the concrete [33]. The reduction of the electrical conductivity with age occurs due to pore filling, which is caused by the continuous formation of the hydration products. The conductivity of OPC mixes is seen to be much higher than those of the PFA and LC3 concrete mixes, in all the cases. This further suggests that there is a limited potential for increasing the ionic resistance of OPC systems by simply reducing the water-binder ratio.

The estimates of m obtained from the evolution of the electrical conductivities (using Eq. (4)) are given in Table 2, in terms of the mean

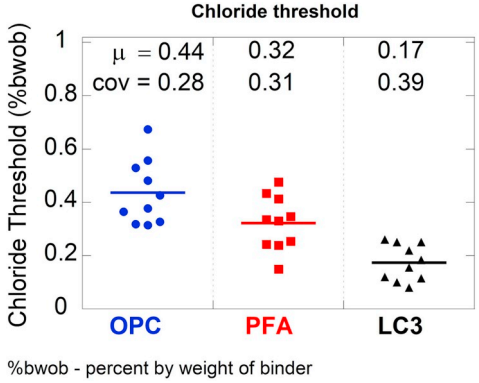

Fig. 5. Chloride threshold for corrosion initiation of the rebar in OPC, PFA and LC3 mortar.

and coefficient of variation. The values obtained for the OPC and PFA concrete are comparable to the ranges reported in the literature [25,35–38]. It can be seen that the ageing coefficients for the OPC concrete are lower than those of the PFA and LC3 systems. Also, the values of m obtained for the LC3 concrete are comparable to those reported for metakaolin mixtures [25,39]. The lower m-values for the OPC concrete can be attributed to the more rapid evolution of the microstructure whereas there is much slower hydration and microstructure evolution in the PFA concrete leading to higher m-values.

4.3. Chloride threshold (Cl_{th})

Fig. 5 shows the Cl_{th}-values obtained for the OPC, PFA and LC3 binders. The highest mean value of Cl_{th} is obtained for OPC (i.e., 0.44% by weight of cement), which reflects the high alkalinity and buffering capacity of $Ca(OH)_2$ at the interface. In the blended systems, the alkalinity is lower due to the consumption of $Ca(OH)_2$ in the pozzolanic reactions and consequently, the Cl_{th}-values obtained for PFA and LC3 systems are less, which is in agreement with the literature [40]. It is to be noted that pozzolanic reactions appear to decrease the Cl_{th} while they increase the ionic resistance and decrease chloride transport, as mentioned earlier.

4.4. Life-cycle assessment

Fig. 6 shows the contribution of the CO_2 emissions arising from different processes and constituents associated with the concrete mixes considered in this study. As expected, the highest contribution is from the binder, with OPC having the highest impact and LC3 having the

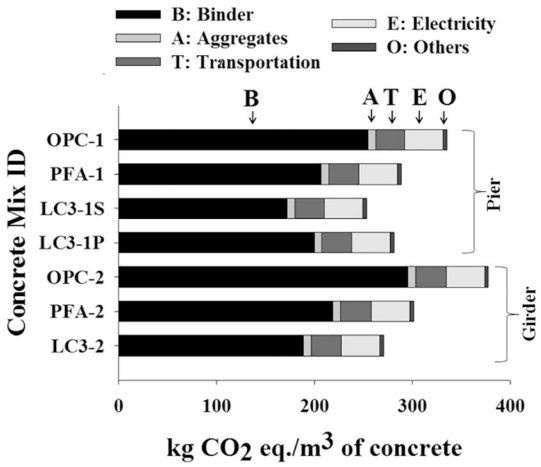

Fig. 6. CO_2 emissions per unit volume of concrete.

least due to their highest and lowest clinker contents, respectively. Note that PFA has been considered here as a waste material from thermal power plants with negligible impact, as is usually done in the cement industry [41,42], though others have advocated the allocation of some impact to the PFA [15,43]. When the binder type is the same, the impact increases with the binder content as in the case of LC3-1P, which has higher binder content, and consequently more CO_2 emissions than LC3-1S and LC3-2. The values given in Table 3 clearly show that the CO_2 emissions in the OPC concrete are significantly higher than those of concrete made with the blended binders. The analysis also indicates that the contributions from other processes and constituents, such as the aggregates, and electricity consumption are almost same in all the cases and that these processes are overshadowed by the cement production process as far as the environmental impact is considered in terms of CO_2 emissions. However, the contribution of transportation can be significant if the LC3 or fly ash is not locally available and has to be transported over a long distance.

5. Illustration of the impact of binders on service life and energy consumption

Two case studies related to typical RC bridges were performed to assess the effect of binder type and concrete proportions on the service life (defined as time to corrosion initiation) and CO_2 emissions per year of service life. The surface chloride concentration (Cl_s) is related to the rate of build-up of chlorides on the concrete surface and the exposure conditions [44,45]; here, the initial and maximum values of Cl_s were considered as 0 and 0.6%bwoc; and the chloride build-up rate was assumed to be 0.04%bwoc per year (considering the location of the bridge to be 800 m away from the ocean, on the Indian coast).

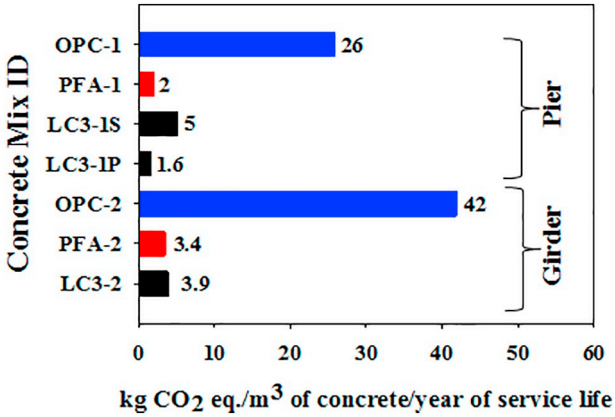

Fig. 8. CO_2-footprint per m^3 and year of service life.

5.1. Case study 1 (bridge pier)

Fig. 7(a) shows the cross-section of the bridge pier under study. The pier is taken to be designed for a characteristic strength of 35 MPa, and consequently any of the M35 category concrete could be considered. When the service life is estimated using the parameters given in Table 2, it yields the CDFs shown in Fig. 7(b) for the four M35 concrete mixes. If we consider a failure probability of 0.5 for comparison, it is seen that the bridge pier with 30% fly ash concrete (PFA-1) can have a service life of approximately 150 years, which is 10 times longer than that of OPC (say, ≈15 years). The data of LC3-1P and LC3-1S indicate that it is possible to design LC3 concrete that can provide similar performance as that of concrete with PFA, despite the Cl_{th} being lower than that of OPC and PFA concrete.

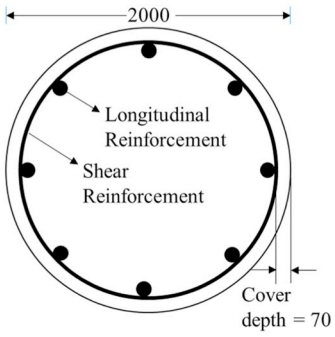

(a) Cross section of bridge pier

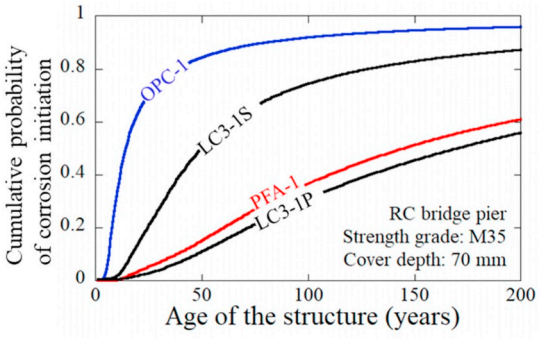

(b) Cumulative distribution function (CDF) of time to corrosion initiation in bridge pier

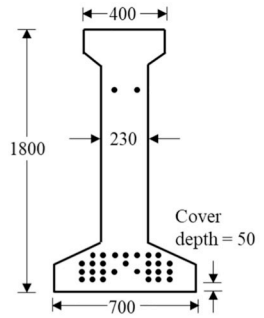

(c) Cross section of bridge girder

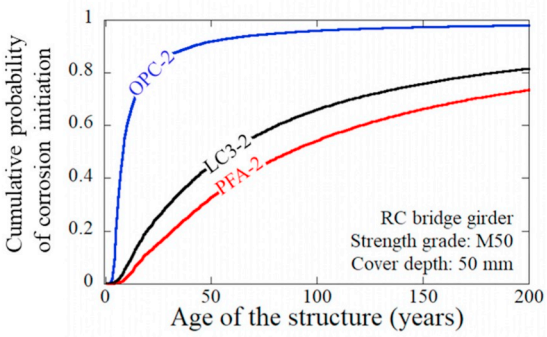

(d) Cumulative distribution function (CDF) of time to corrosion initiation in bridge girder

Fig. 7. Cross section of reinforced concrete elements and estimated service life, defined as time to corrosion initiation, respectively, for the (a, b) pier and (c, d) girder.

As shown in Fig. 8, the emissions per year of service life for LC3-1S concrete are slightly more than that of the PFA-1 concrete, though the emissions per unit volume of the former are lower (see Fig. 6), due to the differences in the estimated service lives. However, the values for both are much lower than that of the OPC-1 concrete. Nevertheless, the annual emissions of LC3-1P (with more binder content) are least because of the longer service life. In summary, Fig. 8 indicates that LC3 mixes can be designed to achieve annual emissions ranging from 1.6 to 5 kg CO_2 eq./m^3 of concrete per year of service life, which is similar to that of PFA systems and significantly lower than that of OPC systems. The difference in the service life estimates clearly emphasizes the role of the binders, such as PFA and LC3, in enhancing durability and lowering the emissions for concrete structures.

5.2. Case study 2 (bridge girder)

Fig. 7(c) shows the cross-section of the RC bridge girder, with a cover depth of 50 mm. The M50 concrete mixes considered in this case study are PFA-2, LC3-2, and OPC-2. Fig. 7(d) shows the CDFs of the corrosion initiation time, which indicates that the girder would have a service life of approximately 10, 60 and 90 years, for the OPC-2, LC3-2 and PFA-2 concrete, respectively, for P_f of 0.5. The potential of concrete made with LC3 in achieving longer service lives than concrete with OPC is substantiated by the results in Fig. 7(d). Also, the total CO_2 emissions per unit volume of LC3-2 mix is lower than that of OPC-2 and PFA-2 mixes. Consequently, the combined effect of the lower clinker content and longer service life of LC3-2 and PFA-2 mixes help in lowering the annual CO_2 emission per year of service life substantially (see Fig. 8).

6. Conclusions

In this study on chloride-induced corrosion in various concrete mixes, the service life parameters such as chloride diffusion coefficient (D_{cl}) and ageing coefficient (m) of the concrete, and chloride threshold (Cl_{th}) of the steel-cementitious interface were determined experimentally and used to estimate the probabilistic service life (conservatively taken as corrosion initiation time) of two concrete categories (M35 and M50). The Cl_{th} and D_{cl} and their synergistic effect on service life should be considered while selecting alternate binders. It is found that the service lives of structures with concrete having PFA and LC3 can be significantly longer than those with only OPC as the binder. Because of the high ionic resistivity, it is possible to design durable concrete with LC3 and PFA, despite the Cl_{th} in such systems being lower than that in OPC systems. Also, the CO_2 footprint per year of service life for PFA and LC3 concrete were found to be much lower than that for the OPC concrete studied. This paper suggests that it is possible to proportion LC3 concrete with (i) higher resistance to chloride ingress and 16% to 30% lower CO_2 footprint than OPC concrete of similar strength, and (ii) similar resistance to chloride ingress and 3% to 12% lower CO_2 footprint than fly-ash based concrete of similar strength.

Acknowledgements

The partial financial support provided by the Swiss Agency for Development and Cooperation through the Climate Change program is gratefully acknowledged. The research work carried out is a part of the Low Carbon Cement project – Phase I led by EPFL, Switzerland. The authors acknowledge the Department of Science and Technology (DST), Government of India and the Ministry of Human Resource Development, Government of India, and the Department of Civil Engineering, Indian Institute of Technology Madras, Chennai, for financial support received. Authors also acknowledge the help of the laboratory staff and students in the Construction Materials Research Laboratory at IIT Madras. The authors thank other members of the Low Carbon Cement project team, especially Prof. K. Scrivener of EPFL, Prof. S. Bishnoi of IIT Delhi, Dr. S. Maity and Mr. V. Rathi of TARA for the productive discussions and suggestions.

References

[1] G.H. Koch, M.P.H. Brongers, N.G. Thompson, Y. Paul Virmani, J.H. Payer, Corrosion Costs and Preventive Strategies in the United States, NACE International, 2002, p. 10.
[2] G. Koch, J. Varney, N. Thompson, O. Moghissi, M. Gould, J. Payer, International Measures of Prevention, Application, and Economics of Corrosion Technologies Study, NACE International, 2016, pp. 1–3 http://impact.nace.org/documents/Nace-International-Report.pdf , Accessed date: 18 July 2018.
[3] B.S. Dhanya, M. Santhanam, Point of view performance specifications for concrete construction in India: are we ready? Indian Concr. J. (2015) 36–43.
[4] M. Alexander, Y. Ballim, M. Santhanam, Performance specifications for concrete using the durability index approach, Indian Concr. J. 79 (2005) 41–46.
[5] M. Antoni, J. Rossen, F. Martirena, K. Scrivener, Cement substitution by a combination of metakaolin and limestone, Cem. Concr. Res. 42 (2012) 1579–1589.
[6] S. Bishnoi, S. Maity, M. Amit, S. Joseph, S. Krishnan, Pilot scale manufacture of limestone calcined clay cement: the Indian experience, Indian Concr. J. 88 (2014) 22–28.
[7] A.C. Emmanuel, P. Haldar, S. Bishnoi, S. Maity, Second pilot production of Limestone Calcined Clay Cement (LC3) in India: the experience, Indian Concr. J. 90 (2016) 57–64.
[8] K.L. Scrivener, Options for the future of cements, Indian Concr. J. 88 (2014) 11–21.
[9] F. Avet, R. Snellings, A. Alujas, K. Scrivener, Development of a new rapid, relevant and reliable (R3) testing method to evaluate the pozzolanic activity of calcined clays, Cem. Concr. Res. 85 (2016) 1–11.
[10] Y. Dhandapani, T. Sakthivel, M. Santhanam, R. Gettu, R.G. Pillai, Mechanical properties and durability performance of concretes with Limestone Calcined Clay Cement (LC3), Cem. Concr. Res. 107 (2018) 136–151.
[11] K. Tutti, Corrosion of Steel in Concrete (Ph.D. Thesis), Lund University, Swedish Cement and Concrete Research Institute, Stockholm, 1982, pp. 1–474 http://portal.research.lu.se/portal/files/4709458/3173290.pdf , Accessed date: 18 July 2018.
[12] U. Angst, B. Elsener, C.K. Larsen, Ø. Vennesland, Critical chloride content in reinforced concrete - a review, Cem. Concr. Res. 39 (2009) 1122–1138.
[13] M. Safehian, A.A. Ramezanianpour, Assessment of service life models for determination of chloride penetration into silica fume concrete in the severe marine environmental condition, Constr. Build. Mater. 48 (2013) 287–294.
[14] M.S. Imbabi, C. Carrigan, S. McKenna, Trends and developments in green cement and concrete technology, Int. J. Sustain. Built Environ. 1 (2012) 194–216.
[15] P. Van Den Heede, N. De Belie, Environmental impact and life cycle assessment (LCA) of traditional and “green” concretes: literature review and theoretical calculations, Cem. Concr. Compos. 34 (2012) 431–442.
[16] H.S. Muller, M. Haist, M. Vogel, Assessment of the sustainability potential of concrete and concrete structures considering their environmental impact, performance and lifetime, Constr. Build. Mater. 67 (2014) 321–337.
[17] I.S. 12269, Ordinary Portland Cement, 53 Grade— Specification, Bureau of Indian Standards, 2013, pp. 1–17.
[18] K.O. Ampadu, K. Torii, M. Kawamura, Beneficial effect of fly ash on chloride diffusivity of hardened cement paste, Cem. Concr. Res. 29 (1999) 585–590.
[19] H.W. Song, C.H. Lee, K.Y. Ann, Factors influencing chloride transport in concrete structures exposed to marine environments, Cem. Concr. Compos. 30 (2008) 113–121.
[20] Y.A. Villagrán-zaccardi, V.L. Taus, Á.A. Di Maio, Time evolution of chloride penetration in blended cement concrete, ACI Mater. J. (2011) 593–601.
[21] ASTM C1556-11a, Standard Test Method for Determining the Apparent Chloride Diffusion Coefficient of Cementitious Mixtures by Bulk Diffusion, ASTM International, 2011, pp. 1–7.
[22] E.J. Gan, P.D. Cady, Condition Evaluation of Concrete Bridges Relative to Reinforcement Corrosion Volume 8: Procedure Manual, Strategic Highway Research Program 8, (1993).
[23] C. Andrade, M. Castellote, R. D'Andrea, Measurement of ageing effect on chloride diffusion coefficients in cementitious matrices, J. Nucl. Mater. 412 (2011) 209–216.
[24] H.S. Al-Alaily, A.A.A. Hassan, Time-dependence of chloride diffusion for concrete containing metakaolin, J. Build. Eng. 7 (2016) 159–169.
[25] M. Nokken, A. Boddy, R.D. Hooton, M.D.A. Thomas, Time dependent diffusion in concrete-three laboratory studies, Cem. Concr. Res. 36 (2006) 200–207.
[26] ASTM-C1760, Standard Test Method for Bulk Electrical Conductivity of Hardened Concrete, ASTM International, 2012, pp. 1–5.
[27] Y. Liu, F.J. Presuel-Moreno, M.A. Paredes, Determination of chloride diffusion coefficients in concrete by electrical resistivity method, ACI Mater. J. 112 (2015) 631–640.
[28] F. Presuel-Moreno, Diffusion vs. Concentration of Chloride Ions in Concrete - Florida Department of Transportation Research Centre Final Report, http://www.fdot.gov/research/completed_proj/summary_smo/fdot-bdk79-977-03-rpt.pdf, (2014) , Accessed date: 18 July 2018.
[29] M.G. Alexander, H. Beushausen, M. Otieno, Corrosion of steel in reinforced concrete: Influence of binder type, water/binder ratio, cover and cracking, Research Monograph No.9 in: Guide to the Use of Durability Indexes for Achieving Durability in Concrete Structures, 2013, pp. 1–77.
[30] D.W. Law, J. Cairns, S.G. Millard, J.H. Bungey, Measurement of loss of steel from reinforcing bars in concrete using linear polarisation resistance measurements, NDT &E Int. 37 (2004) 381–388.
[31] ISO 14040, Environmental Management — Life Cycle Assessment — Principles and Framework, International Organization for Standardization, 2006, pp. 1–20.

[32] R. Gettu, A. Patel, V. Rathi, S. Prakasan, A. Basavaraj, S. Palaniappan, Influence of incorporating supplementary Cementitious materials on the sustainability parameters of cements and concrete in the Indian context, Submitted to Materials and Structures. (personal communications)
[33] Y. Dhandapani, M. Santhanam, Assessment of pore structure evolution in the limestone calcined clay cementitious system and its implications for performance, Cem. Concr. Compos. 84 (2017) 36–47.
[34] Y. Dhandapani, K. Vignesh, T. Raja, M. Santhanam, Development of the microstructure in LC3 systems and its effect on concrete properties, Calcined Clays Sustainable Concrete Proceedings. 2nd International Conference Calcined Clays Sustainable Concreter, 2018, pp. 131–140.
[35] M.D.A. Thomas, P.B. Bamforth, B. Phil, Modelling chloride diffusion in concrete effect of fly ash and slag, Cem. Concr. Res. 29 (1999) 487–495.
[36] H. Justnes, M.O. Kim, S. Ng, X. Qian, Methodology of calculating required chloride diffusion coefficient for intended service life as function of concrete cover in reinforced marine structures, Cem. Concr. Compos. 73 (2016) 316–323.
[37] J.I. Park, K.M. Lee, S.O. Kwon, S.H. Bae, S.H. Jung, S.W. Yoo, Diffusion decay coefficient for chloride ions of concrete containing mineral admixtures, Adv. Mater. Sci. Eng. (2016) 1–11.
[38] K. Stanish, M. Thomas, The use of bulk diffusion tests to establish time-dependent concrete chloride diffusion coefficients, Cem. Concr. Res. 33 (2003) 55–62.
[39] A. Boddy, R.D. Hooton, K.A. Gruber, Long-term testing of the chloride-penetration resistance of concrete containing high-reactivity metakaolin, Cem. Concr. Res. 31 (2001) 759–765.
[40] A. Bentur, N. Berke, S. Diamond, Steel Corrosion in Concrete: Fundamentals and Civil Engineering Practice, E & FN Spon, London, UK, 1997.
[41] CO_2 and Energy Accounting and Reporting Standard for the Cement Industry, Version 3.0, WBCSD - World Business Council for Sustainable Development, 2011, https://www.wbcsdcement.org/pdf/tf1_co2%20protocol%20v3.pdf , Accessed date: 18 July 2018.
[42] The Cement Sustainability Initiative, WBCSD - World Business Council for Sustainable Development, 2012, http://www.csiprogress2012.org/CSI_ProgressReport_FullReport.pdf , Accessed date: 18 July 2018.
[43] C. Chen, G. Habert, Y. Bouzidi, A. Jullien, A. Ventura, LCA allocation procedure used as an incitative method for waste recycling: an application to mineral additions in concrete, Resour. Conserv. Recycl. 54 (2010) 1231–1240.
[44] J. Gergely, J.E. Bledsoe, B.Q. Tempest, I.F. Szabo, Concrete Diffusion Coefficients and Existing Chloride Exposure in North Carolina, 136 North Carolina Dep. Transp., 2006.
[45] A. Costa, A. Appleton, Chloride penetration into concrete in marine environment -part I: Main parameters affecting chloride penetration, Mater. Struct. 32 (1999) 252–259.
[46] Ecoinvent Association, Ecoinvent Database, https://www.ecoinvent.org/database/ecoinvent-33/ecoinvent-33.html , Accessed date: 31 January 2017.
[47] U.S. Environmental Protection Agency, Emission factors for greenhouse gas inventories, http://www.epa.gov/sites/production/files/201512/documents/emissionfactors_nov_2015.pdf, (2015) , Accessed date: February 2018.
[48] PRé Consultants, SimaPro LCA software, version 8.0.5.13, https://Www.Pre-Sustainability.Com/Simapro.